

# Analytical Solutions for Free-Hydrocarbon Recovery using Skimmer and Dual-Pump Wells

Russell T. Johns<sup>1</sup>, Larry W. Lake<sup>1</sup>, Abimbola B. Obigbesan<sup>1</sup>, Leonardo Bermudez<sup>1</sup>, M.R. Hassan<sup>1</sup>, and Randall J. Charbeneau<sup>2</sup>

<sup>1</sup>Petroleum and Geosystems Engineering and

<sup>2</sup>Center for Research in Water Resources

The University of Texas

Austin, Texas 78712-1061

To be published in Groundwater Monitoring and Remediation journal this year....

## Abstract

Accidental release of petroleum hydrocarbons to the subsurface may occur through spills around refineries, leaking pipelines, storage tanks or other sources. If the spill is large, the hydrocarbon liquids may eventually reach a water table and spread laterally in a pancake-like lens. Hydrocarbons that exist as a separate phase are termed light non-aqueous phase liquids (LNAPL). The portion of the LNAPL that is mobile, not entrapped as residual saturation, is termed *free product*.

This paper presents new analytical solutions for the design of long-term free-product recovery from aquifers with skimmer-, single- and dual-pump wells. The solutions are for steady-state flow, based on the assumption of vertical equilibrium, and include the effect of coning of LNAPL, air, and water on flow. The solutions are valid for soils of large hydraulic conductivity where the effect of capillary pressure on coning is small.

The results show how to estimate the maximum rate of inflow of LNAPL for skimmer wells, i.e. wells in which LNAPL is recovered with little or no water production. The paper also shows how to calculate the increase in LNAPL recovery when water is pumped by single or dual-pump wells. A simple equation is given that can be used to adjust the water rate to avoid smearing of the LNAPL below the water table.

## Introduction

Petroleum hydrocarbon products are examples of a “light” non-aqueous phase liquid (LNAPL), which means that they are lighter than and immiscible with water. Being lighter than water, such liquids float on the water table of a groundwater aquifer. Large amounts of spilled petroleum hydrocarbon liquids will depress the 100% water-saturated zone and cause a hydrocarbon liquid lens to spread laterally across the water table in a pancake-like lens. The mobile portion of the LNAPL is known as “free product.” The acronym OIL, which stands for an organic immiscible liquid, is also used to refer to LNAPL.

Effective cleanup of an aquifer requires a) timely removal of LNAPL while b) limiting additional spreading of the contaminant and c) minimizing excessive pumping of the aqueous phase. Lowering the water table near the well can cause the LNAPL to flow into the well. Large rates may cause hydrocarbon to be smeared into soils below the original water table, soils that were perhaps originally uncontaminated. Smearing increases the volume of soil that contains residual hydrocarbon contamination, increasing contamination of the aquifer. Smearing can result in a reduction in the volume of recoverable free hydrocarbon, which may increase long-term remediation costs. Excessive pumping also produces large volumes of water that must be treated and discharged (Fig. 1). Since small water pumping rates may require longer remediation

times, a tradeoff exists between pumping too much water and recovering the LNAPL at too small of a rate.

Many free-product recovery systems in operation employ either single- or dual-pump recovery wells, such as the dual-pump system shown schematically in Fig. 1. Skimmer wells, which produce LNAPL with little or no water production, are also used but these are less efficient than single- or dual-pump wells. Limited guidance is currently available regarding how best to operate these wells for optimum long-term free-product LNAPL recovery (API 1996, Charbeneau *et al.* 1999). As a result, prolonged remediation times and unnecessary expenditures may occur (Charbeneau *et al.* 1999).

Numerical simulation models (Hochmuth and Sunada 1985, Kaluarachchi and Parker 1989, Huyakorn *et al.* 1994, Parker *et al.* 1994, Charbeneau and Chiang 1995) can analyze and design LNAPL migration and recovery. These models usually assume vertical equilibrium of the associated fluids, and simulate LNAPL recovery in two-spatial dimensions rather than in three. These models also include the effect of capillary pressure on coning by accounting for the difference between the floating product thickness observed in monitoring wells and the thickness of porous media containing LNAPL, i.e. the vertical saturation distribution in the soil.

Charbeneau and Chiang (1995) presented an analytical model for calculating free-product recovery rates using a dual-pump system. They also used a vertically averaged numerical simulation model, TWOLAY. TWOLAY assumes segregated water and LNAPL layers with constant saturation and relative permeability values. Delliste *et al.* (1998) and Johns *et al.* (2002) developed analytical models for how capillary pressure affects coning for two-phase flow. Charbeneau *et al.* (1999, 2000) developed comprehensive guidelines for free-product recovery using single- and dual-pump wells. They assumed that the LNAPL thickness is constant with radial distance from the well, an assumption that is strictly valid only for thin LNAPL layers.

In this paper, we present new analytical solutions for estimating recovery of LNAPL by skimmer-, single- and dual-pump wells, in which the thickness of LNAPL, air, and water vary radially. The new analytical model provides benchmark solutions that can be used to test the accuracy of more complicated numerical models (e.g. Kaluarachchi and Parker 1989) that include the effect of capillary pressure on coning. The paper begins by presenting the mathematical model, assumptions, and equations used. The equations and boundary conditions are made dimensionless to generalize the solutions and determine the governing dimensionless groups. We present the solution for two-phase flow of LNAPL and water and limiting forms of the solution. The flow of a skimmer well is such a limiting case. Pumping *windows* are developed that show the physical range of possible LNAPL and water rates for the single- and dual-pump wells. Last, we show how to pump as to avoid smearing of LNAPL below the water table.

## Mathematical Model

Figure 2 illustrates the steady-state downward coning of the phases when only LNAPL and water are flowing. The air phase is assumed to be static. The first subscript on dimensionless thickness  $b$  indicates the phase, whether it is LNAPL ( $o$ ) or water ( $w$ ). The second subscript  $w$  refers to the wellbore and  $i$  refers to the initial layer thickness before flow began, which is constant at the well's radius of influence  $R$ . Fluid is pumped from a vertical wellbore of radius  $r_w$  at a total volumetric flow rate of  $Q_t$ , where  $Q_t = Q_o + Q_w$ . How the thickness of each layer in Fig. 2 varies with radial position is a function of the physical properties of the fluids and soil as well as the phase pumping rates.

The following additional assumptions are made:

- Fluids are incompressible and the fluid viscosities are constant.
- The well produces LNAPL and water at a constant volumetric rate (this is a boundary condition).
- There is one-dimensional radial flow towards the well.
- Fluids are in vertical equilibrium (VE), a condition that causes maximum crossflow of fluids in the vertical direction (Lake 1989). Appendix A discusses the wide applicability of the VE assumption.
- The aquifer is homogeneous and has a constant thickness.
- The aquifer is of sufficient conductivity that capillary pressure is negligible. This assumption implies that the phases flowing are segregated by sharp interfaces, i.e. there are constant but possibly different phase saturations in each layer. Although the saturation within layers is constant, the effect of residual phase saturations on flow is included because each layer has different relative permeabilities.

With these assumptions, the volumetric flow rate at steady-state for phase  $\alpha$  can be written as

$$Q_\alpha = 2\pi r T_\alpha \frac{dh_\alpha}{dr} \dots\dots\dots (1)$$

where the transmissivity is defined as the product of the phase hydraulic conductivity and its thickness,

$$T_\alpha = K_\alpha b_\alpha \dots\dots\dots (2)$$

The parameter  $K_\alpha$  is the effective phase conductivity, which is a function of the relative permeability in the LNAPL or water layer ( $k_{r\alpha}$ ). Because saturation is constant in a layer, i.e. LNAPL at irreducible water saturation, the relative permeability and effective conductivity are also constant within a layer. The effective phase conductivity is given by,

$$K_\alpha = \frac{\rho_\alpha g k k_{r\alpha}}{\mu_\alpha} \dots\dots\dots (3)$$

The phase heads for LNAPL and water,  $h_\alpha$ , are functions of the layer thicknesses  $b_o$  and  $b_w$ . When the reference elevation is the base of the aquifer and the reference pressure is atmospheric pressure, the water head becomes,  $h_w = b_w + \frac{\rho_o}{\rho_w} b_o$ , and the LNAPL head,  $h_o = b_o + b_w$ . Substitution of the expressions for head into Eq. 1 gives the flow equation for the aqueous phase:

$$Q_w = 2\pi K_w b_w \left[ \frac{db_w}{d \ln r} + \frac{\rho_o}{\rho_w} \frac{db_o}{d \ln r} \right] \dots\dots\dots (4)$$

and for LNAPL,

$$Q_o = 2\pi K_o b_o \left[ \frac{db_w}{d \ln r} + \frac{db_o}{d \ln r} \right] \dots\dots\dots (5)$$

Equations 4 and 5 are coupled, because the thickness appearing in each equation depends on the thickness of the other layer. The solution to the coupled equations is subject to the exterior boundary condition (constant thickness at the exterior):

$$\begin{aligned} b_w(r = R) &= b_{wi} \\ b_o(r = R) &= b_{oi} \end{aligned} \dots\dots\dots (6)$$

**Scaling.** In Eqs. 4-6 there are two dependent variables ( $b_w, b_o$ ) and one independent variable ( $r$ ). The dependent variables are a function of ten parameters ( $Q_w, Q_o, K_w, K_o, \rho_w, \rho_o, R, r_w, b_{wi}, b_{oi}$ ) and the independent variable, the radial distance  $r$ . Using scaling analysis, the number of parameters can be reduced by half to only five dimensionless groups ( $Q_{Dw}, Q_{Do}, b_{Dwi}, \rho_D, r_{De}$ ). The equations in dimensionless form are,

$$Q_{Dw} = b_{Dw} \left[ \frac{db_{Dw}}{d \ln r_D} + \rho_D \frac{db_{Do}}{d \ln r_D} \right] \dots\dots\dots (7)$$

and

$$Q_{Do} = b_{Do} \left[ \frac{db_{Dw}}{d \ln r_D} + \frac{db_{Do}}{d \ln r_D} \right] \dots\dots\dots (8)$$

The boundary conditions become

$$\begin{aligned} b_{Dw}(r_D = r_{De}) &= b_{Dwi} \\ b_{Do}(r_D = r_{De}) &= b_{Doi} = 1 - b_{Dwi} \end{aligned} \dots\dots\dots (9)$$

The dimensionless groups in Eqs. 7-9 are related to the ten parameters as follows:

- Dimensionless water flow rate:

$$Q_{Dw} = \frac{Q_w}{2\pi K_w b_{ti}^2}$$

- Dimensionless LNAPL flow rate:

$$Q_{Do} = \frac{Q_o}{2\pi K_o b_{ti}^2}$$

- Density ratio:

$$\rho_D = \frac{\rho_o}{\rho_w}$$

- Dimensionless water thickness at the exterior:

$$b_{Dwi} = \frac{b_{wi}}{b_{ti}}$$

- Dimensionless distance from the well to the exterior:

$$r_{De} = \frac{R}{r_w}$$

The wellbore radius normalizes the independent dimensionless variable,

$$r_D = \frac{r}{r_w} ,$$

and the dependent dimensionless variables are normalized by the initial total thickness, where  $b_{li} = b_{oi} + b_{wi}$ .

That is,

$$b_{Dw} = \frac{b_w}{b_{li}}$$

$$b_{Do} = \frac{b_o}{b_{li}}$$

### Solution of Dimensionless Equations

The exact solution to Eqs. 7-9 is expressed by two equations (see Appendix B for derivation). The first equation relates the dimensionless water thickness to the dimensionless LNAPL thickness at a fixed dimensionless distance:

$$b_{Dw}^2 = b_{Dwi}^2 \left( \frac{v_i + \frac{1}{2} [1 - \varepsilon'] - \frac{\varphi}{2}}{v + \frac{1}{2} [1 - \varepsilon'] - \frac{\varphi}{2}} \right)^{1-\alpha} \left( \frac{v_i + \frac{1}{2} [1 - \varepsilon'] + \frac{\varphi}{2}}{v + \frac{1}{2} [1 - \varepsilon'] + \frac{\varphi}{2}} \right)^{1+\alpha} \dots\dots\dots (10)$$

where,

$$v = \frac{b_{Do}}{b_{Dw}}$$

$$\varepsilon = \frac{Q_{Do}}{Q_{Dw}}$$

$$\varepsilon' = \rho_D \frac{Q_{Do}}{Q_{Dw}}$$

$$\varphi = \sqrt{4\varepsilon + (1 - \varepsilon')^2}$$

$$\alpha = \frac{(1 + \varepsilon')}{\varphi} .$$

The second equation, Eq. 11, expresses LNAPL and water flow into an equivalent one-phase system. That is, the equation is similar to the Dupuit equation (Bear 1979, Charbeneau 2000), which describes the drawdown of water in an unconfined aquifer:

$$Q_{Dt} = \frac{b_{Dti}^2 - b_{Dt}^2}{2 \ln\left(\frac{r_{De}}{r_D}\right)} \dots\dots\dots (11)$$

The total dimensionless rate is

$$Q_{Dt} = Q_{Dw} + \rho_D Q_{Do}$$

and the equivalent total thickness is,

$$b_{Dt}^2 = b_{Dw}^2 + 2\rho_D b_{Do} b_{Dw} + \rho_D b_{Do}^2 .$$

Even though Eqs. 10 and 11 are coupled, they can be solved on a spreadsheet. Solutions are obtained by iterating on  $v$  until a required accuracy is achieved (Delliste *et al.* 1998).

**Two-Phase Flow when  $\rho_D = 1$ .** When the densities of the LNAPL and water are equal, Eqs. 10 and 11 are uncoupled and the solution reduces to a form similar to the Dupuit equation:

$$Q_{Dt} = Q_{Dw} + Q_{Do} = \frac{b_{Dti}^2 - b_{Dt}^2}{2 \ln\left(\frac{r_{De}}{r_D}\right)} \dots\dots\dots (12)$$

where the total equivalent thickness is now the actual total thickness of the LNAPL and water ( $b_{Dt} = b_{Do} + b_{Dw}$ ). Although similar to the Dupuit equation, Eq. 12 is slightly more general because it includes different phase viscosities and relative permeabilities in the dimensionless rates.

**Maximum Fluid Rates When  $b_{Dww} = b_{Dow} = 0$ .** Maximum drawdown at the wellbore occurs when the thicknesses of the water and LNAPL layers at the wellbore are zero. The flow rates of oil and water must now be at their maximum values. For complete drawdown, Eqs. 10 and 11 are uncoupled and the maximum dimensionless rates are,

$$Q_{Dw, \max} = \frac{b_{Dwi}^2 (1 + \rho_D v_i)}{2 \ln r_{De}} \dots\dots\dots (13)$$

$$Q_{Do, \max} = \left( \frac{v_i^2 + v_i}{1 + \rho_D v_i} \right) Q_{Dw, \max} \dots\dots\dots (14)$$

Equations 13 and 14 provide useful mathematical extremes, but achieving complete drawdown is virtually impossible in the field.

**Maximum LNAPL Rate From Skimmer Wells.** Skimmer wells are specially designed to recovery LNAPL, with little or no water ( $Q_{Dw} = 0$ ). The maximum pumping rate of LNAPL occurs when the thickness of the LNAPL is completely drawn down at the wellbore ( $b_{Dow} = 0$ ). For these conditions, Eqs. 10 and 11 reduce to a simple expression for the maximum LNAPL pumping rate in a skimmer well:

$$Q_{Do, \max} = \frac{(1 - \rho_D) b_{Doi}^2}{2 \ln r_{De}} \dots\dots\dots (15)$$

In dimensional form, Eq. 15 becomes

$$Q_{o, \max} = \frac{\pi \left(1 - \frac{\rho_o}{\rho_w}\right) K_o b_{oi}^2}{\ln \left(\frac{R}{r_w}\right)} \dots\dots\dots (16)$$

Equation 16 is similar to the result obtained for coning of water and gas into an oil production well (Pirson 1958).

Once the dimensionless LNAPL rate is determined from Eq. 15, the thickness of the LNAPL and water layers can be calculated. Equations 11 and 12 can be used to approximate the thickness of each phase when a very small water flow rate is specified, i.e.  $Q_{Dw} = 1 \times 10^{-10}$ ; otherwise, the equations are singular at zero water flow rate. For exactly zero water rate, Eqs. 7 and 8 can be integrated to give,

$$b_{Do} = \sqrt{b_{Doi}^2 + \frac{2Q_{Do}}{1 - \rho_D} \ln \left(\frac{r_D}{r_{De}}\right)} \dots\dots\dots (17)$$

and,

$$b_{Dw} = 1 - b_{Doi} - \rho_D (b_{Do} - b_{Doi}) \dots\dots\dots (18)$$

**Maximum Pumping Rates for No Smearing.** It is often desirable (or even regulated) to limit spreading of the LNAPL into previously uncontaminated soil. To avoid this *smearing* of the LNAPL below the initial LNAPL-water interface, the following constraint must be satisfied:

$$\left(\frac{db_{Dw}}{d \ln r_d}\right)_{r_D=r_{De}} \leq 0 \dots\dots\dots (19)$$

Equation 19 states that no smearing will occur when the water thickness at the exterior is either flat or decreasing away from the wellbore. The constraint need only be applied at the exterior because that is where smearing first occurs when the water-pumping rate is increased.

Application of the constraint to Eqs. 10 and 11 (or more easily to Eqs. 4 and 5), gives two possible solutions. The nontrivial solution is,

$$Q_{Do} \geq \frac{b_{Doi}}{\rho_D b_{Dwi}} Q_{Dw} \dots\dots\dots (20)$$

In dimensional form, Eq. 20 becomes,

$$Q_o \geq \frac{\rho_w b_{oi} K_o}{\rho_o b_{wi} K_w} Q_w \dots\dots\dots (21)$$

Equation 20 (or 21) is a very simple, but important result. It shows that the dimensionless oil rate at the limit for no smearing (the equality in Eq. 20) is a linear function of the

dimensionless water rate. Furthermore, Eq. 20 is independent of the well's hydraulic radius of influence ( $R$ ), which makes it more accurate when estimating the optimum pumping rates for no smearing.

## Results and Discussion

Optimal recovery of separate phase hydrocarbon must be defined by the site remediation goals. The goal could be to minimize the amount of residual hydrocarbon left in the formation. However, this may result in small rates of recovery over an extended time. It may also be desirable (or required by regulation) to accelerate the rate of free hydrocarbon removal even though this may result in a reduction in the ultimate recovery of hydrocarbon. Capital, operations and maintenance costs, of course, are always important.

**Dual-Phase Pumping Windows.** Equations 10 and 11 can provide estimates of the water-pumping rate required to maximize LNAPL recovery depending on the site remediation goals. For example, the solution for simultaneous flow of LNAPL and water given by Eqs. 10 and 11 can be used to construct pumping *windows* for the particular contaminated aquifer that describe the permissible limits of the dimensionless rates. Rates outside the pumping window are not physically possible in this segregated model because no additional drawdown of LNAPL and water is possible. Figures 3 and 4 give examples of pumping windows when  $r_{De}$  is 100,  $\rho_D$  is 0.8 (typically value for petroleum hydrocarbons), and  $b_{Doi}$  is 0.2 and 0.1, respectively.

In Fig. 3, point **a** indicates the maximum possible dimensionless LNAPL rate from a skimmer well as calculated by Eq. 15. This rate corresponds to complete drawdown of the LNAPL in the well. It is relatively small compared to the rate that can be obtained if water is also pumped. As water is pumped, the hydraulic gradient of the LNAPL towards the well is increased. The LNAPL thickness also increases. The maximum LNAPL rate, therefore, is increased from that of the skimmer well. This rate follows a curve that goes from point **a** to point **b** and ends at point **c**, which is outside the range of the plot. Along this curve, LNAPL is completely drawn down ( $b_{Dow} = 0$ ). Point **c** corresponds to the maximum possible LNAPL rate as calculated by Eqs. 13 and 14.

The window in Fig. 3 is completed when the curve for complete water drawdown is plotted below the curve for complete LNAPL drawdown. The water drawdown curve (when  $b_{Dww} = 0$ ) begins at point **d**, which corresponds to no LNAPL flow, and ends at point **c**, where the two drawdown curves intersect.

The heights of the LNAPL and water layers at points **a–f** in Fig. 3 are given in Figs. 5–9. Points **a**, **e**, and **f** are at a constant LNAPL rate equal to the maximum skimmer rate. As is shown, rates at points **a**, **e**, and **b** give no smearing of the LNAPL below the original water table. The layers at points **f** and **d**, however, smear.

The size of the pumping window in Fig. 4 is much smaller than that in Fig. 3 because the initial dimensionless LNAPL thickness is smaller (0.2 versus 0.1 in Fig. 4). As expected, the maximum LNAPL rate for a skimmer well is also much smaller in Fig. 4 than in Fig. 3.

**Guidelines to Avoid Additional Smearing.** The pumping window can be used to estimate the required rates to avoid additional smearing into the aquifer. If the water table has fluctuated and residual LNAPL is located below the current water table, Eqs. 10 and 11 can be used to estimate



the flow rates required to avoid additional smearing of LNAPL below soil zones that already contain residual LNAPL.

For the case where there is no residual LNAPL below the current water table, the linear constraint given by Eqs. 20 and 21 apply. Rates in the shaded region in Figs. 3 and 4 give no smearing (dashed-lines are the limit of the constraint). Thus, rates at points **b** and **e** are at the limit for no smearing. Point **b**, however, approximates the optimum because it provides an estimate of the maximum water and LNAPL rates for no smearing.

Figure 10 gives a type curve that can be used to estimate the maximum rates for no smearing (such as point **b**) for different values of initial LNAPL thicknesses and density ratios. The maximum LNAPL rate for a skimmer well is also given in the figure. The increase in the dual-pump LNAPL rate over the skimmer rate varies between 2.0 and 3.0 for density ratios from 0.7 to 0.9. It is relatively independent of LNAPL thickness. For small initial oil thickness, the no smearing water rate may be impracticably small and skimmer pumps will be required (see Fig. 4 where the no-smearing region becomes small).

Equation 21 (or 20) can also be used at the remediation site to adjust the water rates so that smearing does not occur. The procedure would be to first calculate the LNAPL rate based on the equality condition in Eq. 21. If the actual pumping rate is equal or greater to the calculated rate, no smearing probably exists. If the actual LNAPL rate at the well is less than the calculated rate, the water rate should be decreased until Eq. 21 is satisfied. One can continuously adjust the water-pumping rate to satisfy Eq. 21.

## Conclusions

We have developed new analytical solutions to assist in the design of long-term free-hydrocarbon recovery systems when both the water and hydrocarbon (LNAPL) phases are flowing. The new solutions allow for the thickness of the phases to vary with radius. They are valid for soils of large hydraulic conductivity where the effect of capillary pressure on coning is small. These solutions apply to skimmer wells, which are used to collect LNAPL with little or no water production, and to single- and dual-pump wells, where water may be produced separately. Based on the cases examined here, the main conclusions of this research are:

- A skimmer well avoids smearing of the LNAPL below the water table, but the rate of recovery may be small. Pumping the aqueous phase with a single- or dual-pump well may increase the LNAPL recovery rate by a factor of about 2.0 to 3.0 over the skimmer rate, and also avoid smearing.
- Significant increases in the LNAPL rate beyond the factor of 2.0 to 3.0 may be achieved with additional water pumping, but the increased water rate may cause smearing below the water table. This may be acceptable if smearing has already occurred perhaps because of a rising or falling water table.
- Equation 21 (or 20) can be used to estimate the water rate required to avoid smearing. If the LNAPL recovery rate is smaller than expected for the water rate used, the water rate should be decreased until Eq. 21 is satisfied. Equation 21 is easy and practical to use because it is independent of the well's hydraulic radius of influence.

## Acknowledgments

The authors thank the American Petroleum Institute for providing financial support for this research.

## Nomenclature

$A$  = area,  $m^2$   
 $\alpha$  = function of  $\varepsilon$  and  $\varepsilon'$  (see Eq. 10)  
 $b$  = thickness,  $m$   
 $\varepsilon$  = ratio of dimensionless rates (see Eq. 10)  
 $\varepsilon'$  = product of density ratio and  $\varepsilon$  (see Eq. 10)  
 $g$  = gravity constant,  $m/s^2$   
 $h$  = hydraulic head,  $m$   
 $K$  = hydraulic conductivity,  $m/s$   
 $k$  = permeability,  $m^2$   
 $k_r$  = relative permeability at constant saturation  
 $\varphi$  = function of  $\varepsilon$  and  $\varepsilon'$  (see Eq. 10)  
 $\rho$  = density,  $kg/m^3$   
 $q$  = Darcy flow rate,  $m/s$   
 $Q$  = flow rate,  $m^3/s$   
 $R_H$  = aspect ratio  
 $R$  = hydraulic radius of influence,  $m$   
 $r$  = radial distance or coordinate,  $m$   
 $T$  = transmissivity,  $m^2/s$   
 $\mu$  = viscosity,  $Pa \cdot s$   
 $v$  = ratio of dimensionless thicknesses (see Eq. 10)  
 $z$  = elevation from the bottom of the aquifer,  $m$

## Subscripts

$w$  = water (1<sup>st</sup> subscript) or wellbore (2<sup>nd</sup> subscript)  
 $o$  = LNAPL or oil  
 $\alpha$  = phase  
 $D$  = dimensionless variable  
 $i$  = initial value  
 $e$  = area of influence  
 $t$  = total or equivalent

## References

- American Petroleum Institute. 1996. *A Guide to the Assessment and Remediation of Underground Petroleum Releases*, Publication 1628, 3<sup>rd</sup> ed. Washington, D.C.
- Bear, J.: 1979, *Hydraulics of Groundwater*, McGraw-Hill, New York.
- Charbeneau, R.J., Johns, R.T., Lake, L.W. and McAdams, M. 1999. *Free Product Recovery of Petroleum Hydrocarbon Liquids*. American Petroleum Institute, Publication 4682, Washington D.C.
- Charbeneau, R.J. and Chiang, C.Y. 1995. Estimation of Free-Hydrocarbon Recovery from Dual-Pump Systems. *Ground Water* 33, 627-634.
- Charbeneau, R.J., Johns, R.T., Lake L.W., and McAdams, M. 2000. Free Product Recovery of Petroleum Hydrocarbon Liquids. *GWMR*, 147-158, Summer.
- Charbeneau, R.J. 2000. *Groundwater Hydraulics and Pollutant Transport*, Prentice-Hall Inc., Upper Saddle River, NJ.

- Delliste, A.M., Johns, R.T., Lake, L.W., and Charbeneau, R.J. 1998. Effect of Capillary Pressure on Fluid Interfaces. *In Proceedings of Enviromeet '98, Symposium on Environmental Models and Experiments Envisioning Tomorrow*, Irvine, CA.
- Delliste, A.M. 1998. *Steady-State Coning Solutions for Multiphase Flow to a Well*, MS Thesis, University of Texas at Austin, TX.
- Hochmuth, D.P., and Sunada, D.K. 1985. Groundwater Model of Two-Phase Immiscible Flow in Coarse Materials. *Ground Water* 23, 617-626.
- Huyakorn, P.S., Wu, Y., and Park, N.S. 1994. An Improved Sharp-Interface Model for Assessing NAPL Contamination and Remediation of Groundwater Systems. *J. of Cont. Hydrology* 16, 203-234.
- Johns, R.T., Lake, L.W., and Delliste, A.M., Prediction of capillary fluid interfaces during gas or water coning in vertical wells, *SPE Annual Tech. Conf. and Exhib.*, SPE No. 77772, September 29 – October 2, San Antonio, TX, 2002.
- Kaluarachchi, J.J. and Parker J.C. 1989. An Efficient Finite Element Method for Modeling Multiphase Flow in Porous Media. *Water Resour. Res.* 25, 43-54.
- Lake, L.W. 1989. *Enhanced Oil Recovery*, Prentice Hall, Englewood Cliffs, NJ.
- McAdams, M.J. 1997. *Optimization of Free Product Recovery, A Comparison of TWOLAY and UTCHEM*, MS Thesis, University of Texas at Austin, TX.
- Parker, J.C., Zhu, J.L., Johnson, T.G., Kremesec, V.J., and Hockman, E.L. 1994. Modeling Free Product Migration and Recovery at Hydrocarbon Spill Sites. *Ground Water* 32, 119-128.
- Pirson, S. J. 1958. *Oil Reservoir Engineering*, 2<sup>nd</sup> edition, McGraw-Hill, NY.

## Appendix A: Effect of Vertical Equilibrium on LNAPL Recovery

Vertical equilibrium (VE) is a condition that causes maximum crossflow of fluids in the vertical direction (Lake 1989). This appendix derives the criterion that determines when VE is a good approximation.

The easiest way to understand the VE assumption is to write the mass conservation equations for incompressible and steady flow in both the radial ( $r$ ) and vertical ( $z$ ) directions and scale the equations (Lake 1989, Charbeneau *et al.* 1999). The two-dimensional, steady-state mass conservation equations for the air, LNAPL and water phases are

$$\frac{1}{r} \frac{\partial}{\partial r} (r q_{r\alpha}) + \frac{\partial q_{z\alpha}}{\partial z} = 0 \dots\dots\dots (A-1)$$

Substitution of Darcy's law into Eq. A-1 gives

$$\frac{1}{r} \frac{\partial}{\partial r} \left( K_{r\alpha} k_{r\alpha} r \frac{\partial h_\alpha}{\partial r} \right) + \frac{\partial}{\partial z} \left( K_{z\alpha} k_{r\alpha} \frac{\partial h_\alpha}{\partial z} \right) = 0 \dots\dots\dots (A-2)$$

where  $k_{r\alpha}$  is the relative permeability for phase  $\alpha$ ,  $K_{r\alpha}$  is the hydraulic conductivity in the radial direction for phase  $\alpha$ , and  $K_{z\alpha}$  is the hydraulic conductivity in the vertical direction for phase  $\alpha$ . If the independent variables are scaled by

$$r_D = \frac{r}{R}, \quad z_D = \frac{z}{b_{oi}} \dots\dots\dots (A-3)$$

and the hydraulic conductivities are spatially constant, Eq. A-2 can be rearranged as

$$\frac{1}{r_D} \frac{\partial}{\partial r_D} \left( k_{r\alpha} r_D \frac{\partial h_\alpha}{\partial r_D} \right) + R_H^2 \frac{\partial}{\partial z_D} \left( k_{r\alpha} \frac{\partial h_\alpha}{\partial z_D} \right) = 0 \dots\dots\dots (A-4)$$

where the dimensionless aspect ratio  $R_H$  is given by

$$R_H = \frac{R}{b_{oi}} \left( \frac{K_{z\alpha}}{K_{r\alpha}} \right)^{1/2} \dots\dots\dots (A-5)$$

Equation A-4 describes the balance between radial and vertical flow;  $R_H$  determines the balance.  $R_H$  is a ratio of the characteristic time for LNAPL to move across the aquifer in the radial direction to that in the vertical direction. When  $R_H$  is small there is little communication in the vertical direction and the NAPL should experience no drawdown. When  $R_H$  is large, saturation and head fluctuations in the vertical direction decay much faster than those in the radial direction. For large  $R_H$ , therefore, the fluctuations in the vertical direction can be neglected and Eq. A-4 can be written in two parts:

$$\frac{1}{r} \frac{\partial}{\partial r_D} \left( k_{r\alpha} r_D \frac{\partial h_\alpha}{\partial r_D} \right) \approx 0 \dots\dots\dots (A-6)$$

and

$$R_H^2 \frac{\partial}{\partial z_D} \left( k_{r\alpha} \frac{\partial h_\alpha}{\partial z_D} \right) \approx 0 \dots\dots\dots (A-7)$$

Equation A-6 can be integrated to give the steady-state form of Darcy's law, i.e.  $Q_\alpha = q_\alpha A = \text{constant}$ . Equation A-7 can be rewritten as

$$\frac{\partial}{\partial z_D} \left( k_{r\alpha} R_H^2 \frac{\partial h_\alpha}{\partial z_D} \right) \approx 0 \dots\dots\dots (A-8)$$

For large  $R_H$  and finite vertical flow, Eq. A-8 implies that the vertical hydraulic gradient must be small. That is,

$$\frac{\partial h_\alpha}{\partial z_D} \approx 0 \dots\dots\dots (A-9)$$

so that the hydraulic phase gradient is constant vertically, i.e. the fluid potentials are in hydrostatic equilibrium.

Figure 11 gives an example of the two-dimensional steady-state LNAPL flow rate after one year of recovery for different  $R_H$  values simulated with UTCHEM (McAdams 1997). As shown, the LNAPL rate decreases as  $R_H$  increases. The decrease in the LNAPL rate is the result of a reduction in the LNAPL transmissivity near the wellbore as  $R_H$  increases. That is, as VE is approached, LNAPL flows more readily in the vertical direction and the LNAPL layer thickness can be more easily drawn down. For a small or nearly zero  $R_H$ , however, flow is nearly horizontal and the LNAPL layer remains at its initial thickness.

The simulation results in Fig. 11 demonstrate that for the uncertainties in the aquifer properties and geometries, the assumption of VE is valid for an  $R_H$  value greater than 10. A  $R_H$  greater than 10 has been shown by others to be sufficient to ensure that vertical flow is well described by VE for viscously dominated flow (Lake 1989).

Although we have not examined all possible cases here, this work and our previous experience (Lake 1989, McAdams 1997) suggest the following general conclusions:

1. A single dimensionless group, the effective aspect ratio  $R_H$ , scales the vertical equilibrium approximation.
2. VE is a good approximation whenever  $R_H$  is greater than about 10. The other limit, which is absolutely no crossflow, occurs whenever  $R_H$  is less than 0.1. Given typical conditions in most operations, the VE approximation is more nearly satisfied than the no-crossflow limit.
3. Calculations made assuming VE produce smaller NAPL recovery rates than under conditions of no crossflow. Thus, VE estimation is pessimistic in its steady-state recovery prediction.

## Appendix B: Two-Phase Flow Solution

Equations 7 and 8 are solved subject to the exterior boundary conditions given in Eq. 9 and the wellbore boundary condition of constant LNAPL and water flow rate. Division of Eq. 7 by Eq. 8 gives,

$$\frac{Q_{Dw}}{Q_{Do}} = \frac{b_{Dw}}{b_{Do}} \left[ \frac{\frac{db_{Dw}}{d \ln r_D} + \rho_D \frac{db_{Do}}{d \ln r_D}}{\frac{db_{Dw}}{d \ln r_D} + \frac{db_{Do}}{d \ln r_D}} \right] \dots\dots\dots (B-1)$$

After some algebra, Eq. B-1 for a fixed dimensionless distance becomes

$$\frac{db_{Do}}{db_{Dw}} = \frac{\frac{Q_{Do}}{Q_{Dw}} \frac{b_{Dw}}{b_{Do}} - 1}{1 - \frac{Q_{Do}}{Q_{Dw}} \frac{b_{Dw}}{b_{Do}} \rho_D} \dots\dots\dots (B-2)$$

Equation B-2 can be rewritten in terms of the new parameters defined in Eq. 10 as

$$\frac{db_{Do}}{db_{Dw}} = - \left( \frac{v - \varepsilon}{v - \varepsilon'} \right) \dots\dots\dots (B-3)$$

Integration of Eq. B-3 by separation of variables yields the solution presented in Eq. 10. The integral is

$$\int_{b_{Dw}}^{b_{Dwi}} \frac{1}{b_{Dw}} db_{Dw} = \int_v^{v_i} \frac{-1}{\frac{v - \varepsilon}{v - \varepsilon'} + v} dv \dots\dots\dots (B-4)$$

Equation 11 is derived from the definition of the total equivalent flow rate ( $Q_{Dt} = Q_{Dw} + \rho_D Q_{Do}$ ). Substitution of Eqs. 7 and 8 into this definition yields the following expression (after separation of variables)

$$Q_{Dt} d \ln r_D = \frac{db_{Dw}^2}{2} + \rho_D \left( b_{Dw} db_{Do} + b_{Do} db_{Dw} + \frac{db_{Do}^2}{2} \right) \dots\dots\dots (B-5)$$

From the definition of the total equivalent thickness of LNAPL and water (see Eq. 11), Eq. B-5 can be rewritten as

$$Q_{Dt} d \ln r_D = \frac{db_{Dt}^2}{2} \dots\dots\dots (B-6)$$

Integration of Eq. B-6 to the exterior yields Eq. 11.

### Biographical Sketches

**Russell T. Johns** is an associate professor of Petroleum and Geosystems Engineering at the University of Texas at Austin (Department of Petroleum and Geosystems Engineering, University of Texas, Austin, TX 78712-1061, 512-471-1267 (office), 512-471-9605 (fax), rjohns@mail.utexas.edu). He has served on the faculty since 1995 and holds the Pioneer Corporation Faculty Fellowship within the department. He has nine years of industrial experience in both the petroleum and environmental fields with Shell Oil in New Orleans, Houston, and Bakersfield and Colenco Power Consulting in Baden, Switzerland. He holds a Ph.D. degree in petroleum engineering from Stanford in 1992 (with a minor in Water Resources

from civil engineering) and a BS degree in electrical engineering from Northwestern University in 1982. His research interests include theory of gas injection processes, multiphase flow in porous media, remediation of aquifers, and well testing.

**Larry W. Lake** has been a professor of the Department of Petroleum and Geosystems Engineering at the University of Texas at Austin for 24 years. Dr. Lake has authored or coauthored more than 100 technical papers and two textbooks. Dr. Lake is a member of the National Academy of Engineers. He holds the W.A. (Monty) Moncrief Centennial Chair at The University of Texas at Austin.

**Abimbola Obigbesan** was born in Ibadan, Nigeria. He graduated from the University of Lagos, Nigeria with a First Class Honors degree in Chemical Engineering in 1998. He recently completed a Master's degree in Petroleum Engineering at the University of Texas at Austin and is now with ExxonMobil. Apart from environmental remediation, his other research interests lie in enhanced oil recovery by miscible gas injection and risk evaluation in reservoir engineering decisions.

**Leonardo Bermudez** was born in Bogotá, Colombia. He graduated from "Universidad de America" in Petroleum Engineering in 1994. He has working experience spanning over seven years in reservoir management and drilling engineering engaging in under-balanced drilling operations. He is currently pursuing a Master of Science degree in Petroleum Engineering at the University of Texas at Austin. His main research topic is enhanced oil recovery and miscible displacement.

**M.R. Hassan** graduated with a M.S. in petroleum and geosystems engineering from the University of Texas at Austin, where his interests included ground water hydrology and remediation. He is currently a Ph.D. student in ground water hydrology.

**Randall J. Charbeneau** is a professor at the University of Texas at Austin, where he has served on the faculty since 1978. During this period he has been involved with many research projects dealing with migration and fate of hazardous and radioactive materials, ground water modeling, and subsurface remediation. He holds the Jewel McAlister Smith Professorship in Engineering.

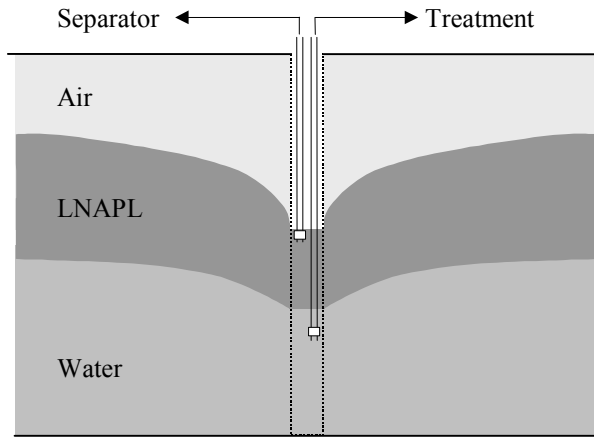


**Fig. 1-** Schematic cross-section of a dual-pump recovery well.

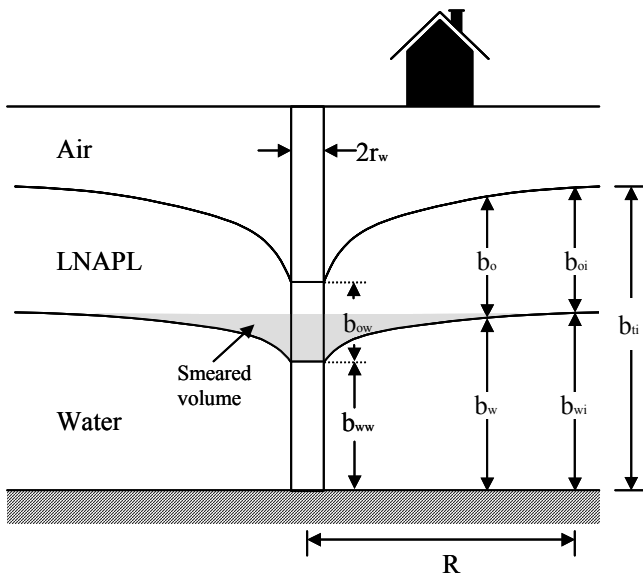


**Fig. 2-** Cross section illustrating steady incompressible radial flow of LNAPL and water phases to a pumping well in an unconfined aquifer. The shaded region shows the volume smeared below the original water table.



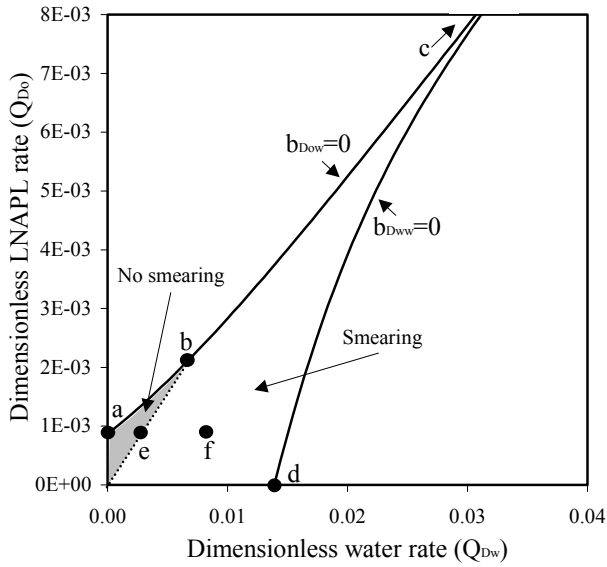


**Fig. 3-** Operational window for dual-phase pumping with  $r_{De} = 100$ ,  $\rho_D = 0.8$ , and  $b_{Doi} = 0.2$ . The shaded region indicates rates that give no smearing. Point **a** is the maximum LNAPL rate from a skimmer well (Eq. 15), **b** gives the maximum rates for no smearing (Eqs. 10, 11, and 20), **c** gives the maximum rates for complete drawdown (Eqs. 13 and 14), and **d** is the maximum water rate with no LNAPL flow.

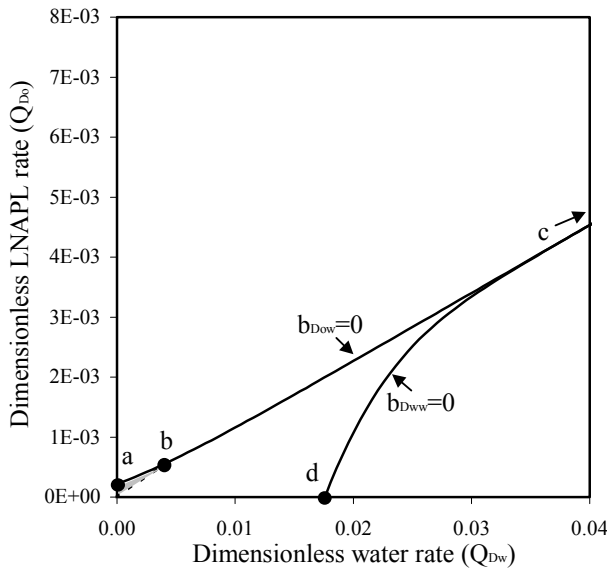


**Fig. 4-** Operational window for dual-phase pumping with  $r_{De} = 100$ ,  $\rho_D = 0.8$ , and  $b_{Doi} = 0.1$ . The no smearing region and the LNAPL rates are smaller compared to Fig. 3.

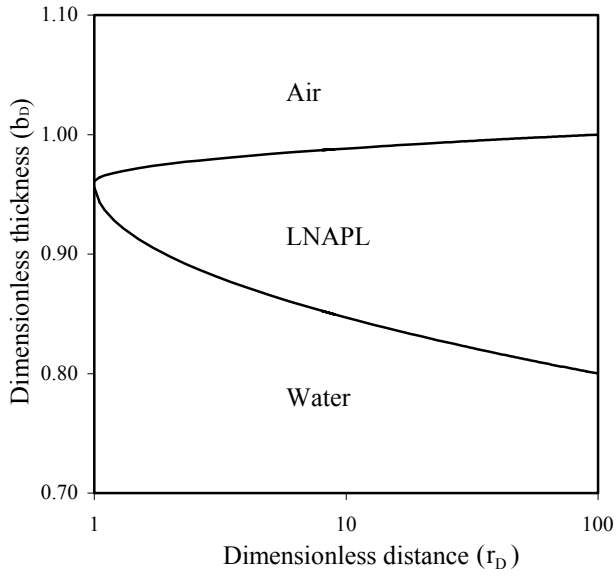


**Fig. 5-** (Case **a** in Fig. 3) Coning of LNAPL and water when LNAPL is pumped from a skimmer well at the maximum rate (Eq. 15) when  $Q_{Dw} = 0$ ,  $Q_{Do} = 8.69 \times 10^{-4}$ ,  $r_{De} = 100$ ,  $\rho_D = 0.8$ , and  $b_{Doi} = 0.2$ .

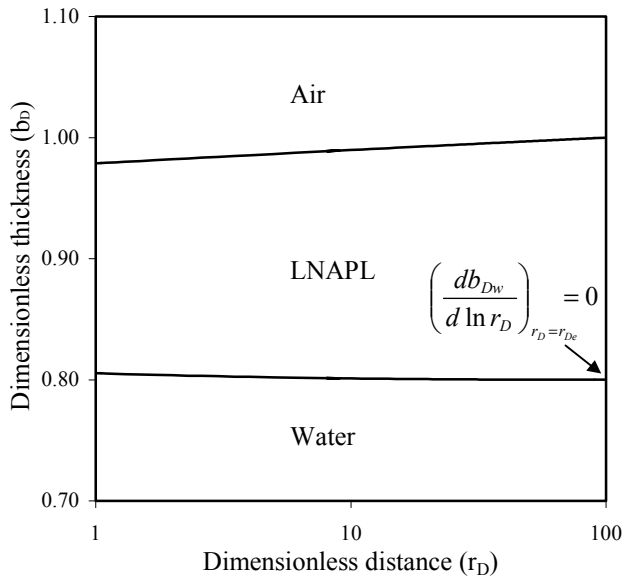


**Fig. 6-** (Case **e** in Fig. 3) Coning of LNAPL and water at the limit of the no-smearing region (Eq. 20) when  $Q_{Dw} = 2.78 \times 10^{-3}$ ,  $Q_{Do} = 8.69 \times 10^{-4}$ ,  $r_{De} = 100$ ,  $\rho_D = 0.8$ , and  $b_{Doi} = 0.2$ .

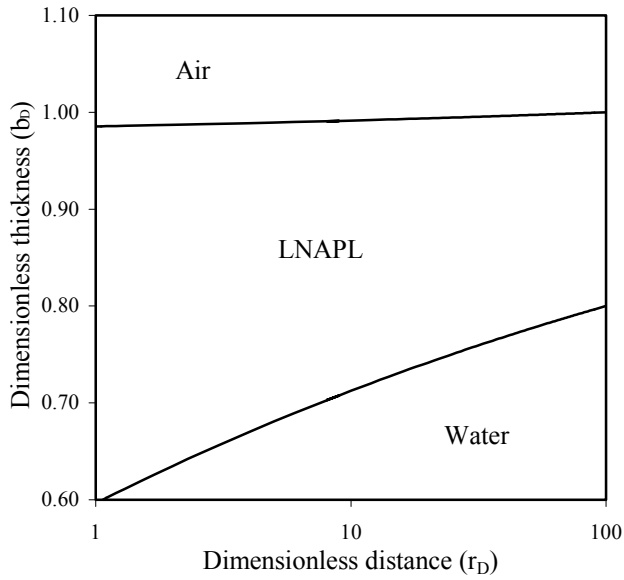


**Fig. 7-** (Case **f** in Fig. 3) Coning of LNAPL and water at the center of the smearing region when  $Q_{Dw} = 8 \times 10^{-3}$ ,  $Q_{Do} = 8.69 \times 10^{-4}$ ,  $r_{De} = 100$ ,  $\rho_D = 0.8$ , and  $b_{Doi} = 0.2$ .

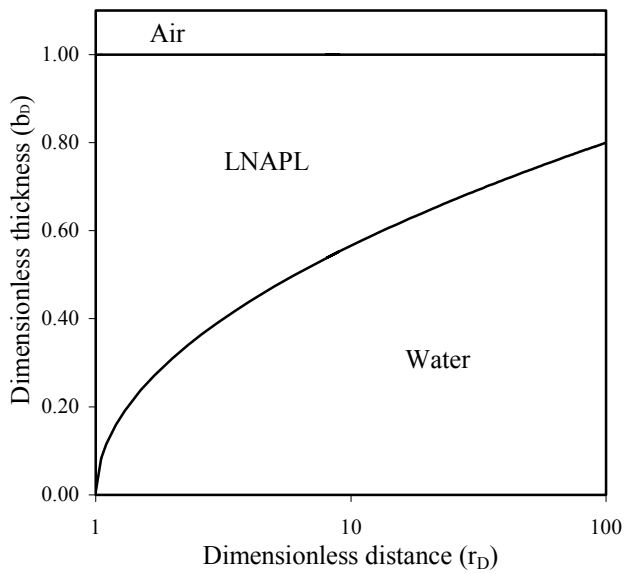


**Fig. 8-** (Case **d** in Fig. 3) Coning of LNAPL and water at the maximum water rate with no LNAPL flow when  $Q_{Dw} = 1.39 \times 10^{-2}$ ,  $Q_{Do} = 0$ ,  $r_{De} = 100$ ,  $\rho_D = 0.8$ , and  $b_{Doi} = 0.2$ .

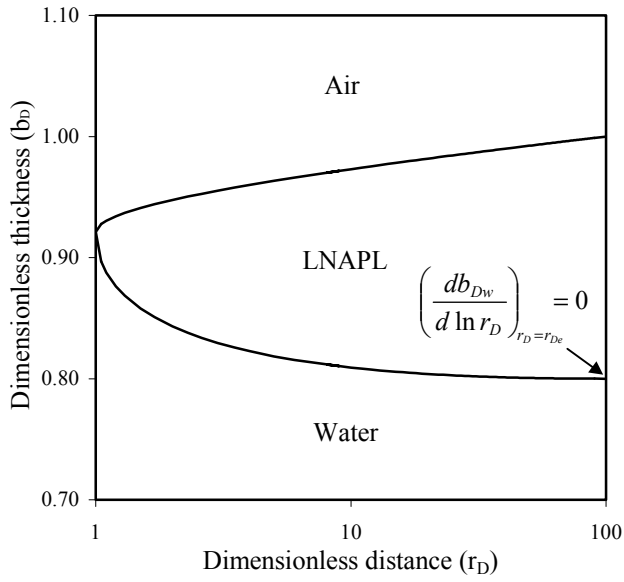


**Fig. 9-** (Case **b** in Fig. 3) Coning of LNAPL and water at the maximum LNAPL and water rates for no smearing (Eqs. 10, 11, and 20) when  $Q_{Dw}= 6.9 \times 10^{-3}$ ,  $Q_{Do}= 2.16 \times 10^{-3}$ ,  $r_{De}= 100$ ,  $\rho_D= 0.8$ , and  $b_{Doi}= 0.2$ .

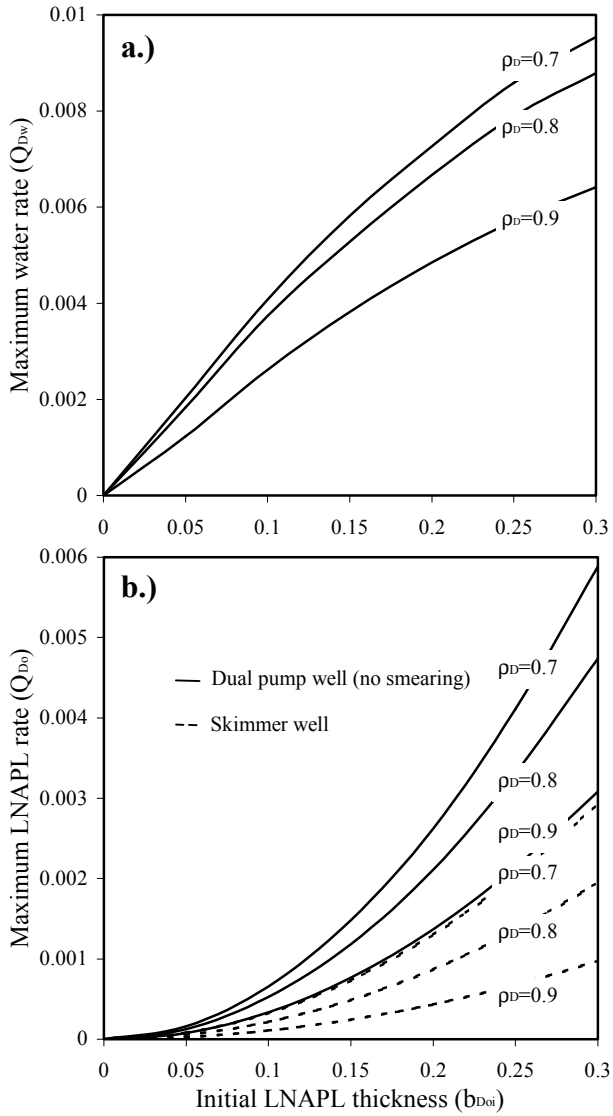


**Fig. 10-** Design curves to estimate maximum a) water and b) LNAPL pumping rates to avoid smearing ( $r_{De} = 100$ ). During pumping, Eq. 20 should be used to adjust rates so that smearing does not occur. The dashed lines are the maximum rates for a skimmer pump when no water is pumped.

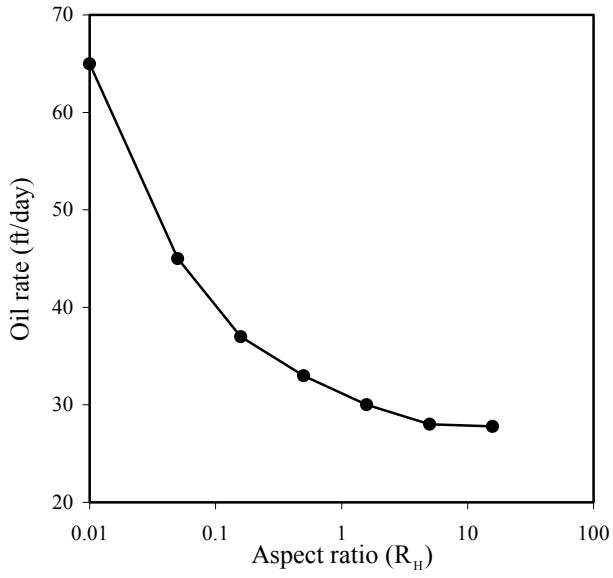


**Fig. 11-** Two-dimensional simulations with UTCHEM showing the effect of the VE assumption on the steady-state LNAPL rate after one year of LNAPL recovery (no capillary pressure).<sup>15</sup>